

GAMMA RAY BURST PREDICTIONS FOR THE FERMI GAMMA RAY SPACE TELESCOPE

TRUONG LE¹ AND CHARLES D. DERMER²
Space Science Division, Code 7653
Naval Research Laboratory, Washington, DC 20375, USA
Accepted for publication in ApJ

ABSTRACT

Results of a phenomenological model to estimate the GRB detection rate by the Fermi Gamma ray Space Telescope are reported. This estimate is based on the BATSE 4B GRB fluence distribution, the mean ratio of fluences measured at 100 MeV – 5 GeV with EGRET and at 20 keV – 2 MeV with BATSE, and the mean EGRET GRB spectrum for the 5 EGRET spark-chamber GRBs. For a 10% fluence ratio and a number spectral index $\alpha_1 = -2$ at 100 MeV – 5 GeV energies, we estimate a rate of ≈ 20 and 4 GRBs per yr in the Fermi Large Area Telescope field of view with at least 5 photons with energy $E > 100$ MeV and $E > 1$ GeV, respectively. We also estimate ≈ 1.5 GRBs per yr in the Fermi FoV where at least 1 photon with energy $E > 10$ GeV is detected. For these parameters, we estimate $\approx 1 - 2$ GRBs per year detected with the Fermi telescope with more than 100 γ rays with $E \gtrsim 100$ MeV. Comparison predictions for $\alpha_1 = -2.2$, different fluence ratios, and the AGILE γ -ray satellite are made. Searches for different classes of GRBs using a diagram plotting 100 MeV – 10 GeV fluence vs. 20 keV – 20 MeV fluence is considered as a way to search for separate classes of GRBs and, specifically, spectral differences between the short-hard and long duration GRB classes, and for hard components in GRBs.

Subject headings: gamma-rays: bursts—theory

1. INTRODUCTION

The Gamma ray Large Area Space Telescope, GLAST, was launched on 11 June 2008 and renamed the Fermi Gamma ray Space Telescope (hereafter Fermi) on August 26, 2008. Fermi comprises two separate instruments, the Large Area Telescope (LAT), which is sensitive to γ rays in the energy range from $E \approx 30$ MeV to $E > 300$ GeV, and the Fermi GLAST Burst Monitor (GBM), sensitive at 10 keV $\lesssim E \lesssim 30$ MeV. At GeV energies, the Fermi LAT provides an increase in effective area over the Energetic Gamma Ray Experiment Telescope (EGRET) on the Compton Gamma Ray Observatory (CGRO) by almost an order of magnitude, a smaller point spread function, a field-of-view (FOV) larger by a factor ≈ 5 than EGRET, and the capability to autonomously slew the LAT in response to a trigger from the GBM. The GBM uses NaI scintillators for triggering, like the Burst and Transient Source Experiment (BATSE), in addition to BGO (Bismuth Germanate) detectors for response in the ~ 0.2 MeV – 25 MeV energy range. The GBM views the unocculted sky, $\approx 50\%$ of the full sky, and the predicted long-duration GBM burst detection rate is $\approx 150 - 225$ per year when triggering using standard BATSE detection criteria ($> 4.5\sigma$ in at least two detectors in 1.024 s in the 50 - 300 keV; Kippen et al. 2001). This can be compared with the BATSE detection rate of ≈ 550 GRBs full-sky brighter than $0.3 \text{ cm}^{-2} \text{ s}^{-1}$ in the 50 - 300 keV band (Band 2002).

Five EGRET γ -ray transients, coincident in time and direction with a BATSE GRB, were detected with the EGRET spark chamber at $E > 30$ MeV with photon counts in excess of background (Dingus 1995). Knowl-

edge from the CGRO can be used to quantify expectations for Fermi. To simulate GRBs in the Fermi energy band, we calculate the average fluence ratio between EGRET (100 MeV – 5 GeV) and BATSE (≈ 20 keV – 2 MeV) from the 5 BATSE GRBs that were detected with the EGRET spark chamber. Using an average spectrum consisting of an empirical Band et al. (1993) spectrum plus a power law, and the effective area of the Fermi LAT, we estimate the full-sky number of GRBs per year with different numbers of high-energy photons based on the BATSE 4B fluence distribution for long-duration GRBs (Paciesas et al. 1999). We make predictions for both long-duration and total GRBs; only the former class of GRBs were convincingly detected at 100 MeV – 5 GeV energies with CGRO. Both Fermi and AGILE view $\approx 1/5^{\text{th}}$ of the full sky at 100 MeV – 5 GeV energies, with the field-of-view defined by the solid angle where the effective area is \gtrsim one-half the on-axis effective area. Thus we consider the realistic detection rate to be $\approx 0.2\times$ the full-sky rate, without considering the potential effects of autonomous repointings in the estimates.

In § 2 we discuss the phenomenological model for GRBs based on BATSE and EGRET data, and estimate the uncertainty in GRB properties derived from EGRET and Fermi measurements. The predicted GRB detection rates and GRB contribution to the diffuse extragalactic background radiation are calculated in § 3. We note that these predictions were made in advance of the launch of Fermi (see arXiv:0807.0355 v1), so can be used to test our knowledge of GRB physics, in particular, whether additional hard, high-energy ($\gtrsim 30$ MeV) γ -ray spectral components are present in GRBs.

2. MODEL

We develop a phenomenological model of GRBs based on the properties of EGRET spark-chamber GRBs, all detected with BATSE, and then make predictions for

¹ tle@ssdl.nrl.navy.mil; now at Space Telescope Science Institute, Baltimore, MD

² charles.dermer@nrl.navy.mil

the GRB detection rate with Fermi and AGILE. Based on BATSE and EGRET results, and from earlier GRB studies, the time-integrated (and resolved, where possible) GRB photon number spectrum $N(E_\gamma)$ is assumed to be well-described by the sum of the Band function (Band et al. 1993), $N_B(\epsilon)$, and a high-energy power law component, $N_G(\epsilon)$. We write this function using dimensionless notation $\epsilon = E_\gamma/m_e c^2$ as

$$N(\epsilon) = N_B(\epsilon) + N_G(\epsilon) \quad (1)$$

where $N_B(\epsilon)$ takes the form

$$N_B(\epsilon) = k_B \epsilon^\alpha \exp[-\epsilon(\alpha - \beta)/\epsilon_{\text{br}}] H(\epsilon; \epsilon_{\text{min}}^B, \epsilon_{\text{br}}) \\ + k_B \epsilon^\beta \epsilon_{\text{br}}^{\alpha-\beta} \exp(\beta - \alpha) H(\epsilon; \epsilon_{\text{br}}, \epsilon_{\text{max}}^B). \quad (2)$$

The parameters α and β are the low- and high-energy Band α and Band β indices, and $E_{\text{br}} = m_e c^2 \epsilon_{\text{br}} \sim 100$ keV is the “break energy.” The photon energy E_{pk} of the peak of the νF_ν spectrum is related to E_{br} through the expression

$$E_{\text{pk}} = \frac{(2 + \alpha)E_{\text{br}}}{\alpha - \beta}, \quad (3)$$

provided $\alpha > -2$ and $\beta < -2$. The Heaviside function is defined such that $H(x; y, z) = 0$ except at $y \leq x \leq z$, where $H(x; y, z) = 1$. The term k_B is the constant normalizing the number fluence to the > 20 keV BATSE energy fluence $\Phi_B (> 20 \text{ keV})$ of a particular GRB, and is given by $k_B = \Phi_B (> 20 \text{ keV})/I_1$, where

$$\frac{I_1}{m_e c^2} = \int_{\epsilon_{\text{min}}^B}^{\epsilon_{\text{br}}} \epsilon^{\alpha+1} e^{-\epsilon(\alpha-\beta)/\epsilon_{\text{br}}} d\epsilon \\ + \epsilon_{\text{br}}^{\alpha-\beta} e^{\beta-\alpha} \int_{\epsilon_{\text{br}}}^{\epsilon_{\text{max}}^B} \epsilon^{\beta+1} d\epsilon. \quad (4)$$

For model GRBs normalized to the BATSE fluence, we take the minimum energy $\epsilon_{\text{min}}^B = 30$ keV, and maximum energy $\epsilon_{\text{max}}^B = 5$ GeV. For the mean GRB spectral indices, we take $\alpha = -0.9$, $\beta = -2.2$, and break energy $E_{\text{br}} = 250$ keV, corresponding to the mean for these values from spectral analyses of bright BATSE GRBs (Preece et al. 2000).

For the high-energy spectral component, we assume that GRBs can be described by a power law at γ -ray energies written as

$$N_G(\epsilon) = k_G \epsilon^{\alpha_1} H(\epsilon; \epsilon_{\text{min}}, \epsilon_{\text{max}}). \quad (5)$$

The average spectrum of GRBs measured by the EGRET spark chamber is $\alpha_1 = -1.95 \pm 0.25$ for 45 γ rays detected within 200 seconds of the trigger (Dingus 1995; Dingus et al. 1998), similar to the average EGRET Total Absorption Shower Counter (TASC) index (Catelli et al. 1998). Band β values for BATSE GRBs have a large range, with most GRBs showing $-2 \lesssim \beta \lesssim 2.5$, but lie in a different range than EGRET and Fermi emissions. The mean spectral index measured by EGRET for the five spark-chamber GRBs is not in good agreement with the index of BATSE and TASC GRBs at $E \gtrsim 1$ MeV (Preece et al. 2000). This suggests that the spectrum is probably not a simple power law at high energies, but different spectral shapes should be considered (e.g., cut-offs or extra components; see Kaneko et al. 2008), and unusual spectral evolution of high-energy components (González et al. 2003).

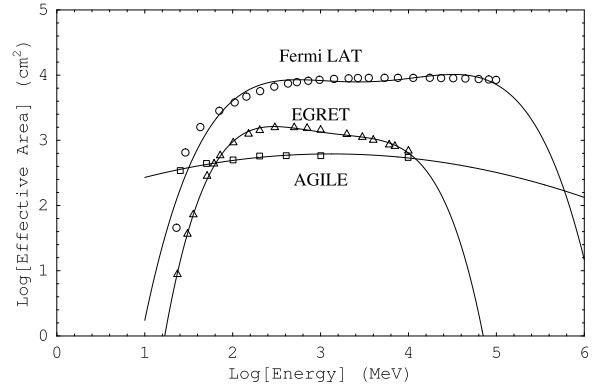


FIG. 1.— Approximate on-axis effective area of the Fermi LAT, EGRET, and AGILE. The symbols are the data, and the solid lines are the best-fitted functions.

Since the spectral index distribution of GRBs at medium γ -ray energies is still debatable, which Fermi will clarify, in this paper we make predictions assuming that the > 100 MeV γ -ray spectrum can be described by a simple power law with $\alpha_1 \cong -2$. For definiteness, we consider $\alpha_1 = -2$ and $\alpha_1 = -2.2$. The latter value corresponds to the softest spectrum within 1σ of the EGRET measurements, and is the same as the Band β used, effectively giving a single power law without break. Besides spectral index, our predictions are also strongly affected by EGRET uncertainties, which we will discuss in the next section.

The term

$$k_G = \frac{\rho \Phi_B (> 20 \text{ keV})}{I_2} \quad (6)$$

where

$$\frac{I_2}{m_e c^2} = \int_{\epsilon_{\text{min}}}^{\epsilon_{\text{max}}} d\epsilon \epsilon^{\alpha_1+1} \quad (7)$$

is the normalization constant based on the average fluence ratio ρ between EGRET and BATSE. In our model, the uncertainties in the number of γ rays that were detected by EGRET and the measured BATSE and EGRET fluences are absorbed into this factor ρ . Here ϵ_{min} and ϵ_{max} are the minimum and maximum energy at 100 MeV and 5 GeV, respectively; note that even though EGRET detected photons down to 30 MeV energies, the effective area dropped rapidly below ≈ 100 MeV. The higher energy given by ϵ_{max} is set by the energy where self-vetoing in EGRET reduces its effective area (see Fig. 1).

The number of source counts with energy $\epsilon > \epsilon_\gamma$ for different detectors (Dermer & Dingus 2004) is given by

$$S_i (> \epsilon_\gamma) \cong f_\gamma \int_{\epsilon_\gamma}^{\infty} A_i(\epsilon) N(\epsilon) d\epsilon, \quad (8)$$

where $A_i(\epsilon)$ is the on-axis effective area of different detectors (e.g., EGRET, Fermi LAT, and AGILE) and f_γ is a collection function depending on the opening angle of the detector. Here we conservatively take the opening angle as energy-dependent with $f_\gamma = 68\%$ containment (Thompson 1986; Dermer & Dingus 2004) though a larger region of interest (ROI) will not much change the results for bright GRBs with many γ rays. The on-axis effective areas for EGRET (A_E), Fermi LAT (A_F),

TABLE 1
EFFECTIVE AREA PARAMETERS

Effective Area (cm ²)	a_0	a_1	a_2	a_3	a_4
A_E	-24.116	36.435	-18.000	3.912	-0.317
A_A	2.010	0.501	-0.080		
A_F	-11.583	18.503	-8.127	1.555	-0.109

and AGILE (A_A) are taken from the best fit to the calibration and analysis data (Pittori et al. 2004; Belli et al. 2007, and references therein) as shown in Fig. 1. The functions describing these areas are

$$\begin{aligned} A_E(x) &= 10^{a_0 + a_1 x + a_2 x^2 + a_3 x^3 + a_4 x^4} \\ A_F(x) &= 10^{a_0 + a_1 x + a_2 x^2 + a_3 x^3 + a_4 x^4} \\ A_A(x) &= 10^{a_0 + a_1 x + a_2 x^2}, \end{aligned} \quad (9)$$

where $x = \log E$, and parameters are given in Table 1. Most GRBs would take place at relatively large angles, $\approx 30 - 60^\circ$, from the Fermi axis, where the effective area is half this value. On the other hand, a larger ROI would include more counts. These represent two additional uncertainties in the rate estimates.

The on-axis effective area of Fermi is shown in Fig. 1. Signal analysis of photon events in the Fermi LAT depends on event reconstruction and background rejection (Atwood et al. 2009). The *diffuse* class of events, for instance, minimizes background by rejecting tracks without good energy measurement in the calorimeter and requires both tracker and calibration information. GRBs can, however, be studied with the *transient* event class, which increases low-energy response at the expense of greater background using large regions of interest around the GRB direction. We consider only photons with $E > 100$ MeV, where the point spread function and consequently the background is smaller than for photons at lower energies, limited at higher energies to a maximum of 5 GeV. Over this energy range, both the EGRET and Fermi effective area is relatively flat, and measurement uncertainty can be more reliably estimated.

3. FLUENCE ESTIMATES AND UNCERTAINTIES FOR EGRET GRBS

In Table 2, we list the pertinent data from EGRET to make estimates of Fermi detection rates. The first five columns of Table 2 give the GRB date-name, the angle of the GRB with respect to the z-axis of the EGRET telescope, the total number and the number of γ rays with energies between 100 MeV and 5 GeV imaged by the EGRET spark chamber, and the maximum γ -ray energy associated with the GRB. With this data, we can calculate the 100 MeV – 5 GeV fluence $F_{0.1-5 \text{ GeV}}$ from an EGRET spark chamber GRB using the expression

$$F_{0.1-5 \text{ GeV}} = \sum_i \frac{E_i}{A(E_i, \theta)}, \quad (10)$$

with the sum being over the $i = 1, \dots, N_\gamma$ γ rays with energies from 100 MeV to 5 GeV detected by the EGRET spark chamber and associated with the GRB, located at the angle θ with respect to the pointing axis of the EGRET.

By choosing a specific energy window between 100 MeV and 5 GeV, we can minimize uncertainty in the

GRB fluence estimate. This is where the EGRET response is best understood, as compared to the higher energy regime with uncertain systematics (Stecker et al. 2008), or at lower energies where the point spread function increases and the numbers of background photons are larger. Because the background photons are more likely to be at low energies, for example, due to difficulties in event reconstruction, the number of background photons, quoted below from the analysis of each specific EGRET GRB, is an upper limit to the number of background photons in the 100 MeV – 5 GeV range.

3.1. Fluence Error Estimate for EGRET Spark Chamber GRBs

Several errors come into the estimate of the 100 MeV – 5 GeV burst fluence, including (i) the statistical error due to the finite number of detected photons; (ii) deadtime effects in the EGRET detector; and (iii) background spark-chamber events erroneously associated with the GRB. Other effects may also play a role, including (iv) errors in energy resolution ($\approx 12\%$ and 9% γ -ray photon energy resolution errors at 100 MeV and 1 GeV, respectively), and (v) errors in effective area. For the EGRET effective area, we use the angle-dependent EGRET effective area with the TASC in coincidence (Fig. 14 of Thompson et al. 1993), where the effective area for the associate burst (See Table 2) is obtained by interpolating the data in Figure 14.

For GRB 910503, 9 photons are detected within 15 s of the GRB trigger, and 6 are likely to be associated with this GRB, implying a possible background of 3 events (Schneid et al. 1992). A 10 GeV γ ray was also detected 84 s after this GRB (Merck et al. 1995) coincident with its location. Six of the γ rays were detected within 2 seconds, allowing as much as a factor of $\approx 30\%$ error for 0.1 s EGRET deadtime if high-energy γ rays are produced roughly uniformly over this time interval. If such emission is produced in bursts shorter than the ~ 0.1 s deadtime, then the GRB produced a stronger fluence than measured. For GRB 910601 (Kwok et al. 1993), 4 events were detected within 100 s of the GRB trigger, with 3 events greater 100 MeV γ rays, when only 1.5 events were expected. This represents a significant uncertainty on the fluence due to background. In contrast, deadtime effects are unlikely to be important for GRB910601 assuming, as we do henceforth, that γ -rays are not produced in sub-100 ms bursts.

GRB 930131, the so-called “superbowl burst,” is interesting in that it shows an intense ~ 0.1 s peak characteristic of a short hard GRB (Sommer et al. 1994), followed ≈ 0.8 s later by a weaker ≈ 0.4 s pulse, and also displays extended emission detected with BATE for 50 s after the GRB trigger (Kouveliotou et al. 1994). Although its $t_{90}(50 - 300 \text{ keV}) = 19.200 \pm 2.56$ s, its $t_{50}(50 - 300 \text{ keV}) = 1.024 \pm 0.091$ s (Paciesas et al. 1999), so it is near the boundary between the long soft and short hard GRBs (Kouveliotou et al. 1993). Note that short hard GRBs are often observed with Swift to produce extended emission (Norris & Gehrels 2008). Sixteen γ rays are imaged within 25 s of the BATSE trigger, of which two pairs and a cluster of three arrive on a sufficiently short, $\lesssim 0.2$ s timescale that deadtime effects could have reduced the detected number of photons. Based on background observed before the trigger time of the GRB, only

TABLE 2
EGRET GAMMA-RAY BURST SPARK CHAMBER DETECTIONS

Burst Date	θ^a	N_{sc}^b	$N_{>100}^c$	$E_{max}(\text{GeV})$	Φ_{BATSE}^d	EGRET GRB γ rays Φ_{EGRET}^e	$\rho(\%)^f$	spectral index of -2 Φ_{EGRET}^e	$\rho(\%)^f$	spectral index of -2.2 Φ_{EGRET}^e	$\rho(\%)^f$
910503	24	9 ^g	2	10	2.92(± 0.01)	1.28	0.43	2.68	0.92	2.20	0.75
910601	12	8	3	0.31	1.5(± 0.01)	1.13	0.75	1.79	1.19	1.48	0.99
930131	28	18	12	1.2	0.66(± 0.11)	26.6	40.3	24.8	37.6	20.3	30.8
940217	10	28	10	18	6.6(± 0.03)	13.0	1.97	5.53	0.84	4.58	0.69
940301	6	7	5	0.16	1.12(± 0.01)	1.14	1.02	2.48	2.21	2.05	1.83

NOTE. — ^a Angle from axis in degrees

^b Number of γ rays imaged by EGRET spark chamber

^c Number of γ rays imaged by EGRET spark chamber between 100 MeV and 5 GeV

^d BATSE 20 keV – 2 MeV fluence, units of 10^{-4} erg cm^{-2} , from Meegan et al. (1996)

^e EGRET 100 MeV – 5 GeV fluence, units of 10^{-6} erg cm^{-2}

^f $\rho = \Phi_{\text{EGRET}}/\Phi_{\text{BATSE}}$

^g Nine events within 15 s after GRB trigger (Schneid et al. 1992)

0.04 events are expected by chance within 25 s (Sommer et al. 1994), so background should not be important for this GRB. This GRB was very intense at BATSE energies, but because most of this emission appeared in a first very short, very intense pulse, the BATSE 20 keV – 2 MeV fluence is smallest of the 5 spark-chamber GRBs.

GRB 940217 (Hurley et al. 1994), with spark-chamber emission extending to > 100 min after the GRB trigger, has associated with it the highest energy photon of all EGRET GRBs, ≈ 18 GeV. A total of 28 γ -ray photons were imaged by the EGRET spark chamber from this GRB, with 10, 8, and 10 appearing during the ≈ 90 s episode of strong BATSE emission, after the BATSE emission and before Earth occultation occurring at ≈ 900 s after the GRB trigger, and after the GRB appears from Earth occultation at ~ 3700 to 5400 s after the GRB. For these three periods, respectively, 0.39, 1.8, and 2.9 background γ rays are expected. Because the GRB was so extended in time and the γ rays arrive one or more seconds apart, deadtime effects can be considered to be small for this GRB. The duration of Earth occultation, representing $\gtrsim 62\%$ of the known period of activity of GRB 940217, therefore represents a major uncertainty in the fluence measurement of this GRB.

Seven photons were imaged within 21 s of the GRB 940301 BATSE trigger (Schneid et al. 1995), though appearing sparsely distributed in time so that deadtime effects are probably negligible. Background is also likely to be small for this GRB, as no other γ rays are detected over a period of 150 s around the time of the GRB except for the 7 photons mentioned.

For completeness, two other GRBs from the CGRO era should be mentioned. This includes GRB 910814, with γ rays observed up to ≈ 50 MeV with the TASC (when the spark chamber was disabled due to Earth occultation; in any case this event was at 38.7° from the EGRET boresight; Kwok et al. 1993). The > 20 keV fluence of GRB 910814 was $\cong 2.51 \times 10^{-4}$ ergs cm^{-2} (Meegan et al. 1996). Late in the CGRO mission, when the EGRET spark chamber gas was mostly depleted, GRB 990123 was observed with COMPTEL to ≈ 18 MeV. This was a bright GRB, with a > 20 keV fluence $\cong 5.1 \times 10^{-4}$ ergs cm^{-2} (Briggs et al. 1999). At redshift $z = 1.6$ (Kulkarni et al. 1999), it provided the first confident lower limits on bulk Lorentz factor using internal $\gamma\gamma$ opacity arguments (Baring 2006). Joint analysis of BATSE and EGRET-TASC GRBs indicates excess, $\gtrsim 1$ MeV emission, though

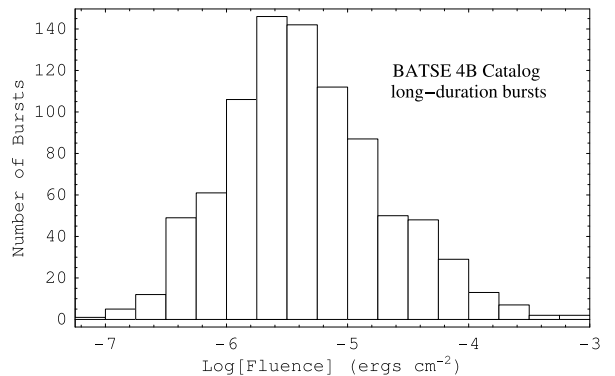


FIG. 2.— Histogram of BATSE 4B catalog GRB fluence distribution; data from Paciesas et al. (1999).

not necessarily extending to $\gtrsim 100$ MeV, in bright, long duration GRBs (González et al. 2009). The > 20 keV fluence of the most notable of these bursts, GRB 941017, was $\cong 3 \times 10^{-4}$ ergs cm^{-2} .

Comparison of the distribution of the fluences of GRBs shown in Fig. 2 in the BATSE 4B catalog with the fluences of the EGRET spark chamber GRBs in Table 2, and notable BATSE-TASC GRBs in the preceding paragraph, shows that the high-energy emission is, for the long duration GRBs, always associated with the most fluent GRBs. This is characteristic of a sensitivity limited detection of high-energy γ -ray emission. Consequently, we can use the increased capabilities of the Fermi telescope with respect to EGRET to make straightforward predictions by scaling from the EGRET results. Note that the weakest GRB in Table 2 in terms of fluence—GRB 930131—is also possibly a short, hard GRB.

3.2. Error from Finite Photon Number

We consider a major error on fluence measurement to result from statistical fluctuations due to the small number of photons imaged by the EGRET spark chamber and associated with the GRB, particularly since we limited the spark chamber events to those with energy between 100 MeV and 5 GeV. It is a simple matter to make this error estimate using a Monte Carlo simulation, and then add other errors to get a complete error estimate.

Let the integrated GRB photon number spectrum be denoted by $dN/dEdA$. The fluence measured between

energies E_1 and E_2 is given by

$$F(E_1, E_2) = \int_{E_1}^{E_2} dE E \left(\frac{dN}{dEdA} \right). \quad (11)$$

The number of source photons is given by

$$N_s(E_1, E_2) = \int_{E_1}^{E_2} dE A(E, \theta) \left(\frac{dN}{dEdA} \right). \quad (12)$$

The probability of detecting a photon of energy E is simply given by inverting the expression

$$r = \frac{\int_E^{E_2} dE A(E, \theta) (dN/dEdA)}{\int_{E_1}^{E_2} dE A(E, \theta) (dN/dEdA)}, \quad (13)$$

for E , where r is a random number uniformly distributed between 0 and 1.

In the EGRET (and Fermi) energy range, $A(E, \theta) \cong \text{const}$ within a factor of ≈ 1.8 for $100 < E(\text{MeV}) < 5000$ and $\theta < 30^\circ$, and can be approximated by a power law over this range, so we write $A(E, \theta) = A_0 E^{-u}$.³ The effect of changing θ on $A(E, \theta)$ over the duration of the GRB is negligible for EGRET, which was a pointing telescope, but can be important in Fermi observations of GRBs. More accurate numerical calculations can be made following the analytic inversion given here.

Assuming that $dN/dEdA \propto E^{-\alpha_1}$, the inversion of eq. (13) is trivial, and we obtain for the detected energy the value

$$E(r) = [E_2^{1-s} + r(E_1^{1-s} - E_2^{1-s})]^{1/(1-s)}, \quad (14)$$

where $s = u + \alpha_1$. The mean photon energy in the energy range $E_1 \leq E \leq E_2$ is

$$\langle E \rangle = \left(\frac{E_1^{2-\alpha_1} - E_2^{2-\alpha_1}}{E_1^{1-\alpha_1} - E_2^{1-\alpha_1}} \right) \left(\frac{\alpha_1 - 1}{\alpha_1 - 2} \right). \quad (15)$$

The error in fluence due to the finite number, N_γ , of photons detected is then given by the root mean square deviation of the detected photon energies from the average photon energy, that is,

$$\Delta E = \sqrt{\frac{\sum_{i=1}^{N_\gamma} [E(r_i) - \langle E \rangle]^2}{N_\gamma}}. \quad (16)$$

The fractional fluence error, $\Delta F/F$, as a function of the number of detected photons $N_\gamma(100 \text{ MeV} - 5 \text{ GeV})$ in the photon energy range between $E_1 = 100 \text{ MeV}$ to $E_2 = 5 \text{ GeV}$ range is shown in Fig. 3 for the simplest approximation of a flat effective area, so that $u = 0$. Because the fluence is weighted by energy, and we have restricted the photon energy to a finite range, a spectrum with $\alpha_1 = 2$ gives the largest fluence uncertainty, which is well described by the function

$$\frac{\Delta F}{F} \cong \frac{1.45}{\sqrt{N_\gamma}}, \quad (17)$$

where that the factor of 1.45 is derived from fitting the data (with $p = 2$) in Figure 3. We can take this expression as providing the maximum error in fluence from

³ See Fig. 1 and www-glast.slac.stanford.edu/software/IS/glast-lat_performance.htm; restricting the photon energies to $> 200 \text{ MeV}$ makes this an excellent approximation.

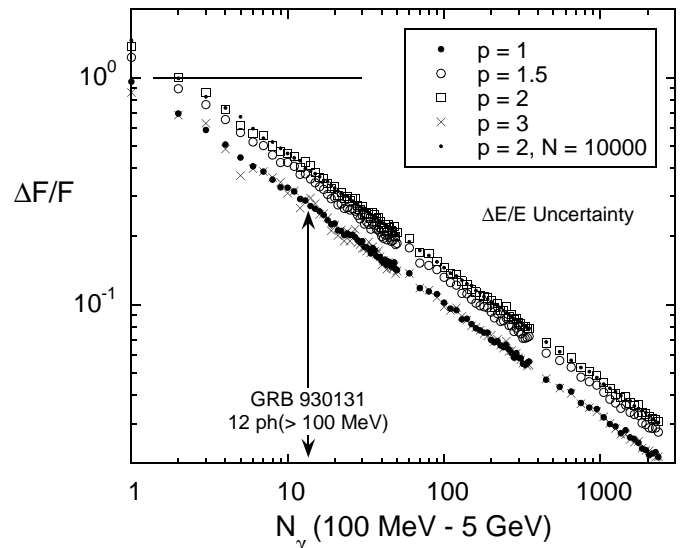


FIG. 3.— Fractional uncertainty in measurement of the 100 MeV – 5 GeV γ -ray fluence due to finite number of photons from the GRB, for an underlying photon spectra described as a power-law with index $\alpha_1 = p$. Calculation uses $N = 1000$ sets of N_γ photons chosen randomly, except where noted.

the statistical uncertainty due to the finite number of photons. If there is a priori knowledge that the intrinsic spectrum has a specific number index, e.g., $\alpha_1 = 2.2$, then the numerical coefficient of eq. (17) becomes rather smaller, ≈ 1.4 . Eq. (17) is a conservative estimate of fluence uncertainty, though it still omits other possible systematic uncertainties. Note that in the EGRET era, GRB 930131 had the largest number of photons, $N_\gamma(100 \text{ MeV} - 5 \text{ GeV}) \approx 12$, γ rays, in the 0.1 – 5 GeV range. As is apparent from Fig. 3, finite photon number gives the major source of error to the fluence measurement of EGRET spark-chamber GRB.

In comparison, the error associated with relative energy uncertainty is, as already noted, at the $\approx 10\%$ level for EGRET. For the Fermi Gamma ray Space Telescope, the relative energy uncertainties at photon energies of 0.1, 1, and 10 GeV are $\approx 17\%$, 9% , and 8% for normal incidence, and $\approx 15\%$, 9% , and 5% at 60° off-axis (Atwood et al. 2009). Because this can be a calibration uncertainty affecting all photon energy measurements systematically rather than statistically, this uncertainty on the fluence will start to dominate for those rare GRBs detected with Fermi with more than ~ 50 photons between 100 MeV and 5 GeV. Effective area uncertainties also appear at the $\sim 10\%$ level. Consequently, the uncertainty from the finite number of photons dominates fluence measurement for EGRET GRBs.

From the discussion of EGRET GRBs in Section 3.1 and their properties in Table 2, we can now reliably estimate the fluence uncertainty associated with finite number of photons, background and deadtime effects measured with EGRET in the 0.1 – 5 GeV energy range. For GRB 910503, we take $N_\gamma(100 \text{ MeV} - 5 \text{ GeV}) = 2$, essentially giving 100% uncertainty in the measurement of fluence (taking twice this value would give a 2σ upper limit). For GRB 910601, we again conservatively take $N_\gamma(100 \text{ MeV} - 5 \text{ GeV}) = 2$ in view of possible background. For GRB 930131, we take $N_\gamma(100 \text{ MeV} - 5 \text{ GeV}) = 12$, keeping in mind that a deadtime correction

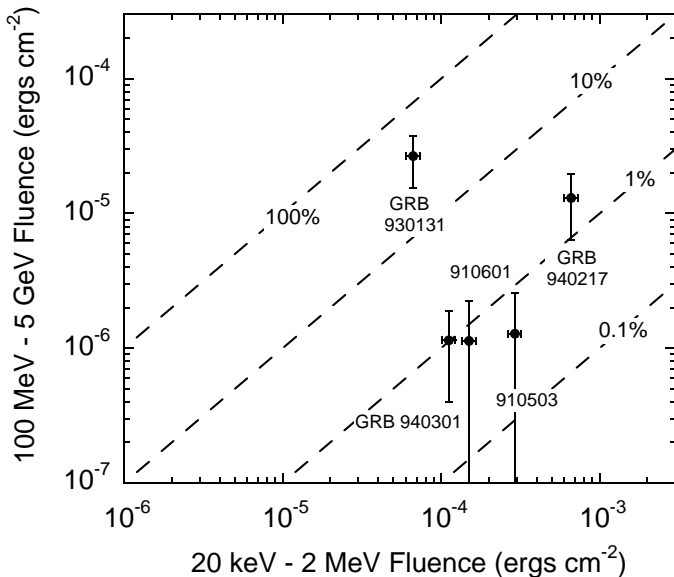


FIG. 4.— Diagram plotting fluence measured between 100 MeV and 5 GeV with the EGRET spark chamber vs the 20 keV – 2 MeV fluence measured with BATSE for the 5 EGRET spark chamber GRBs. The EGRET fluence for GRB 940217 could easily be a factor of two larger due to Earth occultation during the active phase of this GRB.

in the absolute fluence by tens of percent or more could be required, depending on the distribution of γ -ray arrival times, which Fermi will measure. For GRB 940217, we take $N_\gamma(100 \text{ MeV} - 5 \text{ GeV}) = 8$, subtracting two background photons that could have contributed during the first prompt and early afterglow in this GRB (note that no EGRET photons in the 100 MeV – 5 GeV range were detected after Earth occultation). For GRB 940301, we take $N_\gamma(100 \text{ MeV} - 5 \text{ GeV}) = 5$.

3.3. Fluence Estimate from EGRET Photon Event List

The statistical errors associated with the finite number of detected photons, being the largest source of error for the EGRET GRBs, are used with the values in Table 2 and eq. (10) to produce Fig. 4. This figure displays the 100 MeV – 5 GeV fluence measured with the EGRET spark chamber vs. the 20 keV – 2 MeV fluence measured with BATSE. Bolometric corrections to a larger energy range are usually small if E_{pk} , the peak photon energy of the νF_ν spectrum, falls in this waveband. This is not always the case for these GRBs, and comparison of this figure with reported results in the Fermi era must consider bolometric corrections.

This fluence-fluence diagram provides, potentially, one way to discriminate between different classes of GRBs on the basis of their γ -ray radiative efficiency. A much more accurate comparison will be provided for those GRBs with known redshift. Because deadtime and background effects have been corrected from these EGRET spark chamber GRBs, the fluence-fluence diagram gives a picture where the long-duration GRBs have a radiative efficiency ρ in $> 100 \text{ MeV}$ γ rays of $\approx 1\%$ or a few % of the bolometric energy output. Assuming no class bias in the values in Table 2, these give the average deduced radiative efficiency $\langle \rho \rangle \cong 9\%$ (column 8). This suggests that we use as a mean fluence ratio a number between ≈ 10 , before considering broad ranges of value of ρ or even separate classes with different ρ values.

4. ALTERNATE FLUENCE ESTIMATE

As a check on ρ , we also make an independent estimate using the number $N_\gamma(> 100 \text{ MeV})$ of $> 100 \text{ MeV}$ γ -ray photons that were detected by EGRET (Dingus 1995), assuming a hard component of the spectrum with spectral indices $\alpha_1 = -2$ and $\alpha_1 = -2.2$. The EGRET fluence in the energy range of 100 MeV to 5 GeV can be expressed as

$$\Phi_{\text{EGRET}} = N_\gamma(> 100 \text{ MeV}) \frac{\int_{100 \text{ MeV}}^{5 \text{ GeV}} E^{1-\alpha_1} dE}{\int_{100 \text{ MeV}}^{5 \text{ GeV}} E^{-\alpha_1} A(E, \theta) dE}, \quad (18)$$

where $A(E, \theta)$ is the angle-dependent EGRET effective area obtained by interpolating the data in Figure 14 of Thompson et al. (1993). From Table 2 we find that the average measured fluence ratios ρ for the 5 spark chamber bursts are $\rho \approx 9\%$ (column 10) and $\rho \approx 7\%$ (column 12) for spectra indices of $\alpha_1 = -2$ and -2.2 , respectively. This is consistent with our previous estimate of $\approx 9\%$, because that referred to the $> 100 \text{ MeV} - 5 \text{ GeV}$ fluence to 20 keV–2 MeV fluence ratio, rather than the $> 30 \text{ MeV} - 5 \text{ GeV}$ fluence to 20 keV–2 MeV fluence ratio, the latter of which is expected to be $\approx 50\%$ larger. However, these average fluence values of 9% and 7% are dominated by the boundary of long-soft and short-hard GRB 930191 with the fluence ratios of 40% and 30% for spectra indices of -2 and -2.2 , respectively. Four other bursts are long GRBs with the average fluence ratios of 1.3% and 1%. Hence, we expect the average fluence for the long GRBs to be larger, conservatively, we assume values of 5% and 4% for spectra indices of $\alpha_1 = -2$ and -2.2 , respectively, to represent long-duration GRBs.

However, as previously noted, the total γ -ray flux is probably larger than EGRET measured. The γ -ray emission from GRB 940217 (Hurley et al. 1994) likely persisted during the period of Earth occultation, easily increasing the number of photons by ~ 2 . Deadtime effects, as seen in GRB 930131 (Sommer et al. 1994), could have caused the number of γ rays to be undercounted. Besides, there is the example of GRBs with anomalous hard tails, like GRB 990104 (Wren et al. 2002) and GRB 941017 (González et al. 2003), the latter with fluence in the $\approx 1 - 100 \text{ MeV}$ range comparable to or greater than the sub-MeV fluence. Further, there is the low-significance Milagrito detection of the X-ray flash-type GRB 970417a (Atkins et al. 2003), which would not only have to be at low redshift $z \lesssim 0.3$ but also have much greater TeV than MeV fluence. Hence we expect the average fluence ratios ρ between EGRET and BATSE to be $\approx 10\%$ and $\approx 8\%$ for spectra indices of $\alpha_1 = -2$ and $\alpha_1 = 2.2$, respectively.

We use $\rho = 0.1$ for model with $\alpha_1 = -2$ and $\rho = 0.08$ for model with $\alpha_1 = -2.2$ to define the value of k_G . The estimated total number of long-duration GRBs that get detected by any detectors are based on the BATSE 4B fluence distribution (Paciesas et al. 1999), shown in Fig. 2, assuming an annual GRB rate of 670 GRB/yr, including untriggered GRBs with photon fluxes smaller than $0.3 \text{ cm}^{-2} \text{ s}^{-1}$ (Band 2002). The BATSE 4B Catalog contains 1292 bursts total, including short and long duration GRBs. There are a total of 872 long-duration GRBs that are identifiable in the BATSE 4B Catalog. When we estimate the number of source counts over one

TABLE 3
FERMI AND AGILE GRBs/YR FOV ($\approx 1/5^{th}$) PREDICTIONS

Threshold Energy	spectral index of -2		spectral index of -2.2	
	Fermi	AGILE	Fermi	AGILE
> 30 MeV (> 5 photons)	30 ^a (18) ^b	7 ^a (4) ^b	12 ^c (6) ^d	2 ^c (< 1) ^d
> 100 MeV (> 5 photons)	20 (12)	2 (< 1)	8 (4)	< 1 (< 1)
> 1 GeV (> 5 photons)	4 (< 2)	< 1 (0)	< 1 (0)	< 1 (0)

NOTE. — This column has value with fluence ratio of ^a10%; ^b5%; ^c8%; ^d4%.

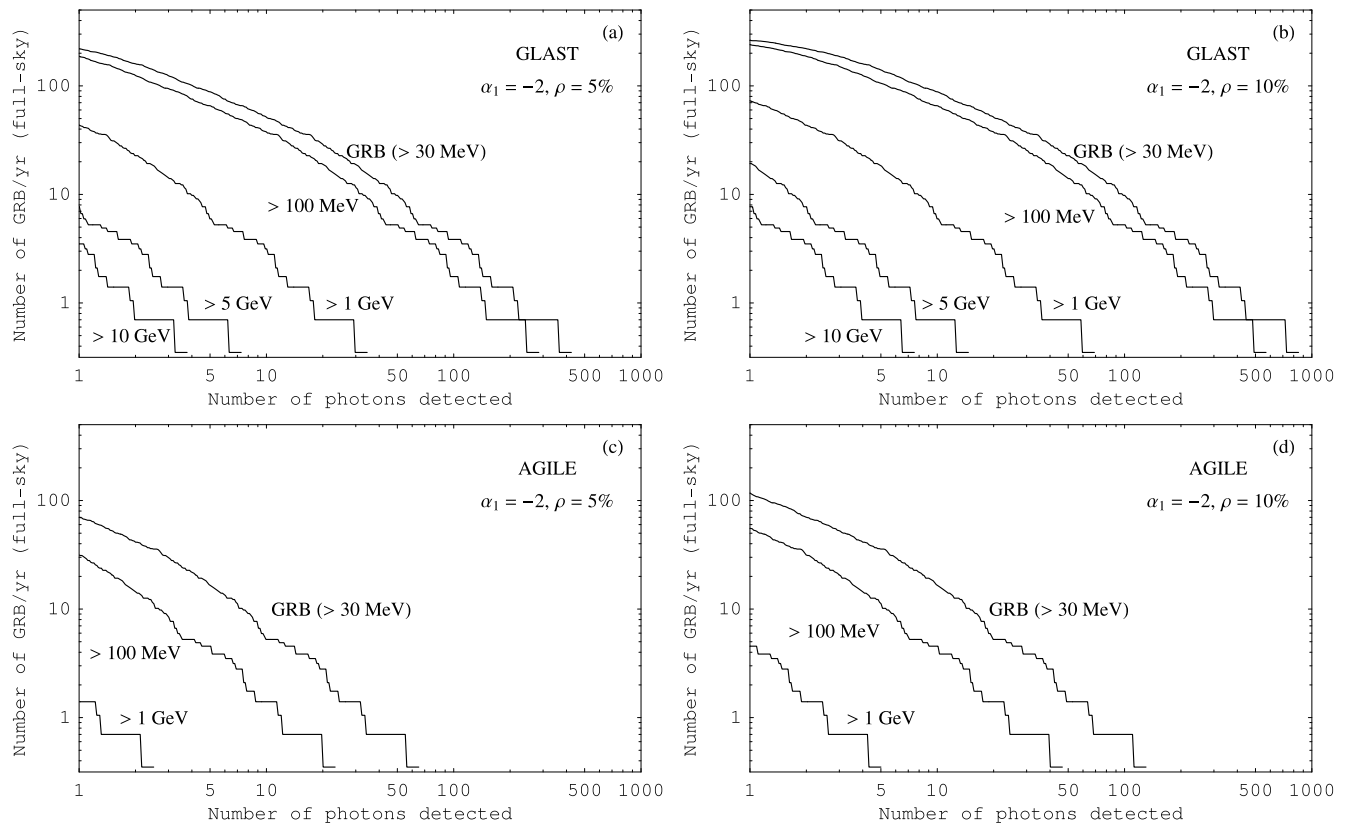


FIG. 5.— Prediction for the number of long-duration GRBs per year full-sky Fermi LAT (a and b) and AGILE (c and d) will see based on a measured fluence ratio extrapolated from a -2 photon spectrum from EGRET/BATSE to EGRET LAT energies. The curves describe the burst rate assuming a -2 photon spectra for different energy thresholds.

year period, the ratio 872/1292 is applied to represent the long-duration GRB predictions.

5. RESULTS

In Figs. 5 and 6, we plot full-sky Fermi LAT and AGILE GRB detection rates, assuming that the Band-spectrum extends to $\gtrsim 100$ MeV energies. This simple model predicts that $\approx 30, 20$, and 4 GRBs will be observed per year with the Fermi LAT with at least 5 photons with energies $E > 30$ MeV, $E > 100$ MeV, and $E > 1$ GeV, respectively. This is assuming a hard spectral index $\alpha_1 = -2$ and a fluence ratio $\rho = 10\%$. For $\alpha_1 = -2.2$, the model predicts that $\approx 12, \approx 8$, and probably no GRBs per year should be detected with at least 5 photons with $E > 30$ MeV, $E > 100$ MeV, and $E > 1$ GeV, respectively, now assuming that $\rho = 8\%$.

The analysis also predicts that ≈ 7 and ≈ 2 GRBs per year with at least 5 photon counts at $E > 30$ MeV and $E > 100$ MeV, respectively, should be detected by

AGILE assuming $\alpha_1 = -2$ and $\rho = 10\%$ (see Fig. 5d). For $\alpha_1 = -2.2$, the model predicts that ≈ 2 and probably no GRBs with at least 5 photons with $E > 30$ MeV and $E > 100$ MeV, respectively, will be detected by AGILE per year with $\rho = 8\%$ (see Fig. 6d). A consistently smaller number of GRBs/yr full-sky is predicted for both Fermi and AGILE for the steeper spectral indices, as expected. In Table 3, we summarize the predicted number of GRBs per yr with at least 5 photons greater than a specific γ -ray photon energy in the FoV, ≈ 2.5 sr, of the Fermi LAT and AGILE, considering GRBs with hard spectral indices $\alpha_1 = -2$ and $\alpha_1 = -2.2$, and for fluence ratios $\rho = 10\%, 8\%, 5\%$, and 4% .

These models assume that all GRBs have power law with $\alpha_1 \approx -2$ and 10% fluence ratio or -2.2 and 8% fluence ratios, and these assumptions would be first to be examined if Fermi LAT shows strong violations of these predictions. For $\alpha_1 = -2$ and $\rho = 10\%$, we estimate from Fig. 5 that $\approx 1 - 2$ GRBs per year will be detected with

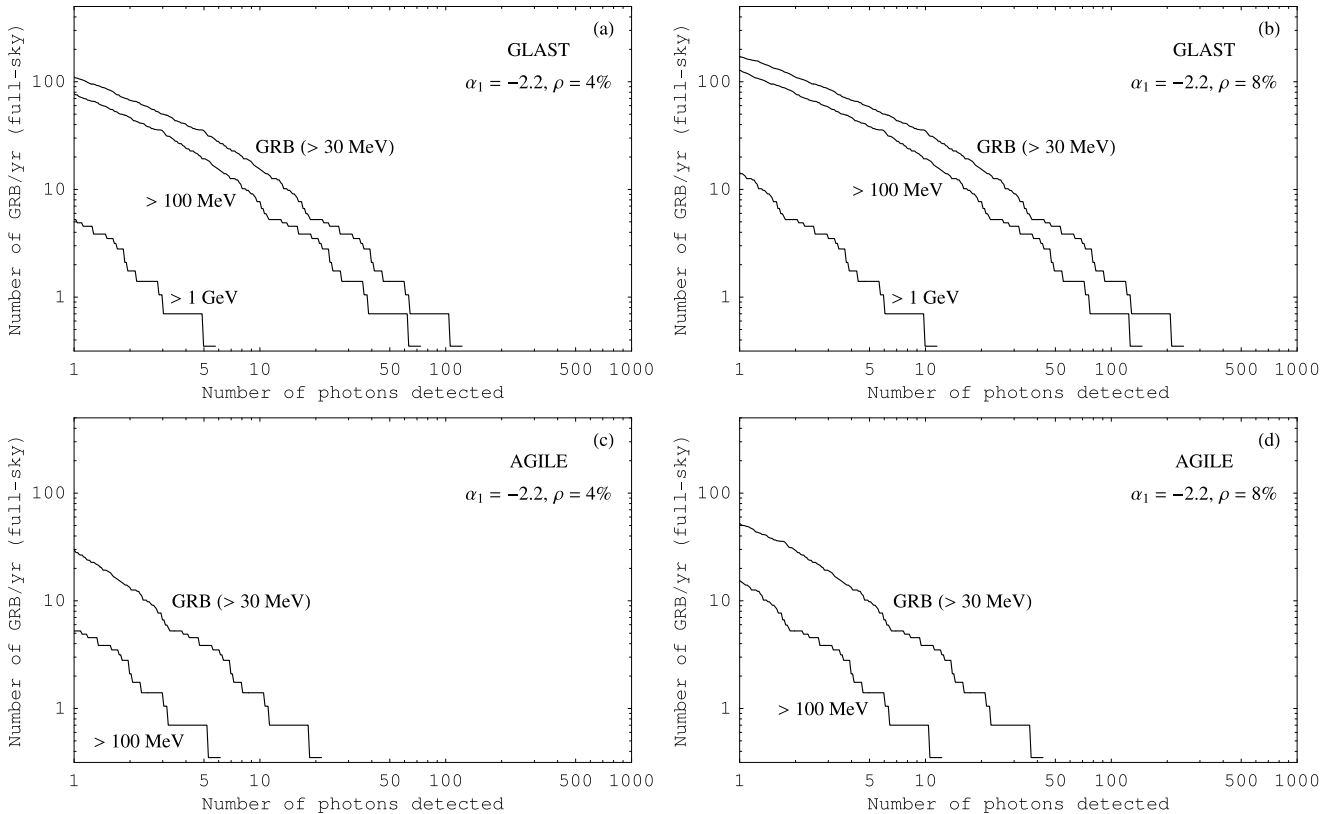


FIG. 6.— Prediction for the total number of GRBs/yr full-sky that Fermi LAT (a and b) and AGILE (c and d) will detect for GRB spectra as described in Fig. 3 for an assuming -2.2 photon spectra.

the Fermi telescope that have more than 100 γ rays with $E \gtrsim 100$ MeV. The models also predicts that the GBM fluences of long-duration GRBs detected with the LAT should be large, $\gtrsim 10^{-5}$ ergs cm^{-2} . The distribution of fluences can be compared with predicted distributions for Swift and the Fermi GBM (Le & Dermer 2007).

From this treatment of the fluence ratio, we can estimate the diffuse extragalactic γ -ray background produced by GRBs using the 4B BATSE fluence catalog based on the EGRET/BATSE fluence ratio. From the 4B Catalog there are a total of 1292 GRBs, of which 872 bursts are long-duration GRBs. The total average fluence for the long-duration GRB is about $\approx 1.40 \times 10^{-2}$ ergs cm^{-2} . Assuming 670 GRBs/yr, we estimate that less than 1% of the diffuse extragalactic γ -ray background could come from GRBs assuming $\approx 8\%$ or 10% fluence ratio. Unless there is a large class of $\rho \approx 1$ GRBs, which were not found with the EGRET spark chamber, this suggests that GRBs gives very little contribution to the diffuse extragalactic γ -ray background (e.g., Dermer 2006; Casanova et al. 2007).

6. CONCLUSIONS

As we enter the Fermi era, it is worthwhile to make final predictions based on results from the EGRET CGRO era. Here we have adopted an approach making use of mean fluence ratios in the EGRET 100 MeV – 5 GeV and BATSE 20 keV – 2 MeV bandpasses. Obviously this already introduces significant K-corrections when calculating the intrinsic properties of the GRB sources; a sample of GRBs with known redshifts is clearly preferred.

Nevertheless, we fix the fluence ratios in these bands to obtain straightforward predictions for all-sky detection rates with Fermi, using on-axis effective areas and the BATSE 4B fluence distribution. Multiplication by $1/5^{\text{th}}$ gives the final detection rate with the Fermi LAT tracker and calorimeter (Atwood et al. 2009)

For a 10% fluence ratio and a hard component with -2 index, we estimate $\approx 1 - 2$ per month with more than 5 photons with $E > 100$ MeV γ rays in the LAT FoV, and 1 or 2 per year with more than 100 γ rays with $E > 100$ MeV. A bright GRB for spectral modeling, with more than ≈ 100 photons with $E > 100$ MeV, is predicted once or twice per year. We note that with the use of -2 fluence spectrum, the detection of a > 10 GeV photon from a GRB is considered very improbable, barring the existence of an additional component harder than -2 .

Furthermore, as the Fermi GBM and the Fermi LAT instruments begin to collect data from GRBs, we recommend to plot LAT fluence vs. GBM fluence and, more importantly, mean LAT GRB spectral index vs. LAT/GBM fluence ratios ρ to search for distinct classes of GRBs distinguished by their high-energy properties.

We thank David Band, Michael Briggs, Valerie Connaughton, Brenda Dingus, Magda González, Chryssa Kouveliotou, Julie McEnery and Nicola Omodei for many interesting discussions and useful suggestions, and especially to Nicola Omodei and Julie McEnery for a really difficult and constructive report. We also thank the referee for comments, corrections, and useful suggestions. The work of CD is supported by the Office of

Naval Research and NASA Fermi Science Investigation at the Naval Research Laboratory.
 DPR-S-1563-Y, which also supported the research of TL

REFERENCES

- Atkins, W. B., et al. 2003, *ApJ*, 583, 824
 Atwood, R., et al. 2009, *ApJ*, to be submitted
 Band, D., et al. 1993, *ApJ*, 413, 281
 Band, D. L. 2002, *ApJ*, 578, 806
 Baring, M. G. 2006, *ApJ*, 650, 1004
 Belli, F. et al. 2007, *Nuclear Instruments and Methods in Physics Research*, A570, 276
 Briggs, M. S., et al. 1999, *ApJ*, 524, 82
 Casanova, S., Dingus, B. L., & Zhang, B. 2007, *ApJ*, 656, 306
 Catelli, J. R., Dingus, B. L., & Schneid, E. J. 1998, *American Institute of Physics Conference Series*, 428, 309
 Dermer, C. D., 2006, in *The Multi-Messenger Approach to High-Energy Gamma-Ray Sources*, eds. J. M. Paredes, O. Reimer, and D. F. Torres (New York: Springer), 127
 Dermer, C. D. 2007, *ApJ*, 659, 958
 Dermer, C. D., & Dingus, B. L. 2004, *New Astr. Rev.*, 48, 537
 Dingus, B. L. 1995, *Ap&SS*, 231, 187
 Dingus, B. L., Catelli, J. R., & Schneid, E. J. 1998, *American Institute of Physics Conference Series*, 428, 349
 González, M. M., Dingus, B. L., Kaneko, Y., Preece, R. D., Dermer, C. D., & Briggs, M. S. 2003, *Nature*, 424, 749
 González, M. M., et al. 2009, *ApJ*, submitted
 Hurley, K., et al. 1994, *Nature*, 372, 652
 Kaneko, Y., González, M. M., Preece, R. D., Dingus, B. L., & Briggs, M. S. 2008, *ApJ*, 677, 1168
 Kippen, R. M., et al. 2001, *Gamma 2001: Gamma-Ray Astrophysics*, 587, 801
 Kouveliotou, C., Meegan, C. A., Fishman, G. J., Bhat, N. P., Briggs, M. S., Koshut, T. M., Paciesas, W. S., & Pendleton, G. N. 1993, *ApJ*, 413, L101
 Kouveliotou, C., et al. 1994, *ApJ*, 422, L59
 Kulkarni, S. R., et al. 1999, *Nature*, 398, 389
 Kwok, P. W., et al. 1993, *American Institute of Physics Conference Series*, 280, 855
 Le, T., & Dermer, C. D. 2007, *ApJ*, 661, 394
 Meegan, C. A., et al. 1996, *ApJS*, 106, 65
 Merck, M., et al. 1995, *IAU Colloq. 151: Flares and Flashes*, 454, 358
 Norris, J. P., & Gehrels, N. 2008, *American Institute of Physics Conference Series*, 1000, 280
 Omodei, N., & for the GLAST/LAT GRB Science Group 2006, *astro-ph/0603762*
 Paciesas, W. S., et al. 1999, *ApJS*, 122, 465
 Pittori, C., Tavani, M., & AGILE Team 2004, *Bulletin of the American Astronomical Society*, 36, 929
 Preece, R. D., Briggs, M. S., Malozzi, R. S., Pendleton, G. N., Paciesas, W. S., & Band, D. L. 2000, *ApJS*, 126, 19
 Schneid, E. J., et al. 1992, *A&A*, 255, L13
 Schneid, E. J., et al. 1995, *ApJ*, 453, 95
 Sommer, M., et al. 1994, *ApJ*, 422, L63
 Sreekumar, P., et al. 1998, *ApJ*, 494, 523
 Stecker, F. W., Hunter, S. D., & Kniffen, D. A. 2008, *Astroparticle Physics*, 29, 25
 Strong, A. W., Moskalenko, I. V., & Reimer, O. 2004, *ApJ*, 613, 956
 Thompson, D. J., et al. 1993, *ApJS*, 86, 629
 Thompson, D. J. 1986, *NIM Physics Research A*, 251, 390
 Wren, D. N., Bertsch, D. L., & Ritz, S. 2002, *ApJ*, 574, L47